

Photochromic silver nanoparticles fabricated by sputter deposition

J. Okumu

Department of Physics, Kenyatta University, P.O. Box 43844, Nairobi, Kenya

C. Dahmen^{a)} and A. N. Sprafke

I. Physikalisches Institut (IA), Lehrstuhl für Physik neuer Materialien, Rheinisch-Westfälische Technische Hochschule (RWTH) Aachen, 52056 Aachen, Germany

M. Luysberg

Institut für Festkörperforschung (IFF)/ Forschungszentrum Jülich, 52428 Jülich, Germany

G. von Plessen and M. Wuttig

I. Physikalisches Institut (IA), Lehrstuhl für Physik neuer Materialien, Rheinisch-Westfälische Technische Hochschule (RWTH) Aachen, 52056 Aachen, Germany

(Received 16 September 2004; accepted 16 February 2005; published online 19 April 2005)

In this study a simple route to preparing photochromic silver nanoparticles in a TiO₂ matrix is presented, which is based upon sputtering and subsequent annealing. The formation of silver nanoparticles with sizes of some tens of nanometers is confirmed by x-ray diffraction and transmission electron microscopy. The inhomogeneously broadened particle-plasmon resonance of the nanoparticle ensemble leads to a broad optical-absorption band, whose spectral profile can be tuned by varying the silver load and the annealing temperature. Multicolor photochromic behavior of this Ag–TiO₂ system upon irradiation with laser light is demonstrated and discussed in terms of a particle-plasmon-assisted electron transfer from the silver nanoparticles to TiO₂ and subsequent trapping by adsorbed molecular oxygen. The electron depletion in the nanoparticles reduces the light absorption at the wavelength of irradiation. A gradual recovery of the absorption band is observed after irradiation, which is explained with a slow thermal release of electrons from the oxygen trapping centers and subsequent capture into the nanoparticles. The recovery can be accelerated by ultraviolet irradiation; the explanation for this observation is that electrons photoexcited in the TiO₂ are captured into the nanoparticles and restore the absorption band. © 2005 American Institute of Physics. [DOI: 10.1063/1.1888044]

INTRODUCTION

Photochromic materials reversibly change their color under illumination. They have been suggested for a wide range of applications including information storage¹ and large-scale displays.² Silver halide photochromic glasses were reported as early as 1964.³ Two other classes of inorganic photochromic materials have been widely studied: rare-earth-doped glasses^{4,5} and thin films of transition-metal oxides.^{6,7}

Recently, multicolor photochromism was reported in nanocomposite Ag–TiO₂ films. These films consist of Ag nanoparticles embedded in anatase TiO₂ and were prepared photocatalytically using the sol-gel technique.^{8,9} Here, the photochromic effect relies on reversible spectral hole burning in the particle-plasmon band of the particles. Particle plasmons are collective oscillations of conduction electrons and generally show themselves as pronounced resonances in optical spectra of metal nanoparticles. The photochromic effect adds an interesting new aspect to the rich optical behavior known from Ag nanoparticles and clusters, such as light scattering and absorption,¹⁰ nonlinear signal enhancement,¹¹ electroluminescence,¹² and photoactivated fluorescence.¹³ The anatase phase of TiO₂ is a well-known photocatalytic

material; it is chemically stable and optically transparent.¹⁴ Chemical, such as sol gel,^{15,16} and physical, such as ion implantation and cosputtering,^{17–19} techniques have been used to deposit noble metals in TiO₂ for various applications.

Naoi *et al.*⁹ have suggested several applications, including rewritable or electronic paper, for the photochromic Ag–TiO₂ films, once they can be easily prepared and applied to large areas. These requirements are typically best met by films deposited using magnetron sputtering. Films obtained by magnetron sputtering are used for a wide range of applications.²⁰ In this paper, we report on magnetron-sputtered Ag–TiO₂ films with photochromic functionalities. Ag nanoparticles are formed in a TiO₂ matrix by sequentially sputtering from Ag and Ti targets and annealing the resulting films. The Ag particles that are formed during the thermal treatment are characterized using x-ray diffraction and transmission electron microscopy. The particles, whose sizes are some tens of nanometers, lead to a broad optical-absorption band across the visible range. The mechanisms of photochromic changes in response to visible and ultraviolet light are studied. Spectral holes are burned into the absorption band by irradiation with laser light of different wavelengths. The spectral hole burning is discussed in terms of plasmon-assisted electron transfer from the silver nanoparticles into the TiO₂ conduction band and electron trapping by adsorbed molecular oxygen, resulting in an electron depletion in the

^{a)}Electronic mail: cdahmen@physik.rwth-aachen.de

nanoparticles. The spectral hole can be removed by capture of electrons from the TiO₂ conduction band into the nanoparticles.

EXPERIMENT

Ag–TiO₂ nanocomposite films were deposited on glass, silicon, and quartz substrates by direct current (dc) magnetron sputtering. In a first step, an amorphous TiO₂ layer was deposited by sputtering a Ti target at a constant pressure of 1 Pa and a cathode current of 900 mA in an oxygen–argon atmosphere. Then a Ag target was sputtered in a pure-argon atmosphere at a total pressure of 0.8 Pa and a cathode current of 170 mA. The amount of silver sputtered was varied between film thickness equivalents of 6 and 15 nm; these film thickness equivalents were determined by sputtering directly onto a glass substrate under otherwise identical conditions and measuring the thickness of the resulting Ag film using x-ray reflectometry. Subsequently, a second TiO₂ layer was sputtered under the conditions given above. All the sputtering processes took place at a background pressure of 10^{−6} mbar. Unless stated otherwise, the total TiO₂ film thickness sputtered was 60 nm. For comparison, we also prepared pure TiO₂ films under identical conditions.

The Ag–TiO₂ films deposited on glass and quartz were subjected to x-ray diffraction (XRD) and optical characterization, respectively. The films were then heated to various temperatures at a heating rate of approximately 10 °C/min in an argon atmosphere; they were subsequently annealed for 1 h at this temperature. Grazing incidence x-ray diffraction ($\lambda=1.542$ Å) analysis was performed to determine the structure of the films. Transmission electron microscopy (TEM) was employed on Ag–TiO₂ films deposited on Si substrates to confirm the formation of Ag nanoparticles in the TiO₂ matrix and to determine the lateral size of these nanoparticles. For the optical characterization of the films, transmittance and reflectance were measured before and after laser irradiation. Spots with areas of 3–5 mm² were irradiated using a blue-green Argon-ion laser ($\lambda=488$ nm), a green neodymium-doped yttrium vanadate (Nd:YVO₄) laser ($\lambda=532$ nm), and a red helium–neon laser ($\lambda=633$ nm) in ambient air in a dark room. The optical transmittance $T(\lambda)$ and reflectance $R(\lambda)$ of the illuminated spots were determined immediately after laser illumination. The absorbance $A(\lambda)$ of the spots was calculated using the relation²¹ $A(\lambda)=1-T(\lambda)-R(\lambda)$. These spots were optionally illuminated with light from an ultraviolet lamp (Hanau Fluotest, $\lambda=365$ nm).

RESULTS AND DISCUSSION

Nanoparticle formation

The grazing incidence XRD scans of the nanocomposite films (Fig. 1) illustrate the state of the silver in the various stages of film treatment. The lowest graph shows the XRD scan performed on the as-deposited sample. The only prominent feature is the broad shoulder around 26° corresponding to the amorphous TiO₂ matrix. Apparently, the silver present inside the system is finely dispersed in the amorphous TiO₂ matrix. In contrast, Ag peaks are clearly visible in the XRD

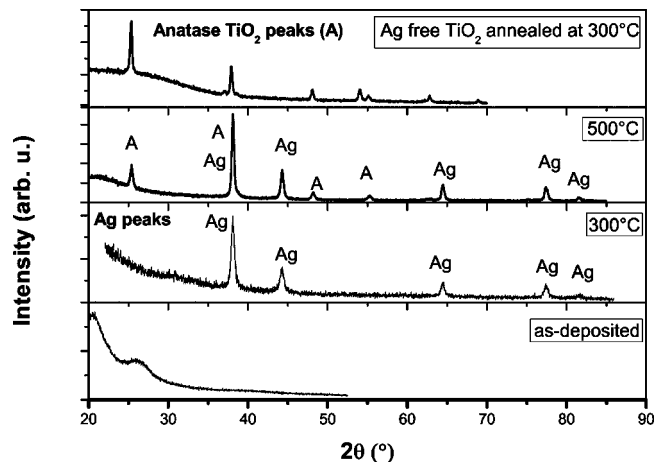


FIG. 1. Grazing incidence x-ray diffraction scans of Ag–TiO₂ films (Ag film thickness equivalent: 12 nm) and a Ag-free TiO₂ film. In the as-deposited film, no silver peaks are evident, which indicates that the silver is finely dispersed in the amorphous TiO₂. Upon annealing, silver nanoparticles are formed and peaks (Ag) can be observed in the XRD profiles. Annealing at 500 °C results in the crystallization of the TiO₂ into the anatase phase (A). Pure TiO₂ (top scan) films already exhibit anatase peaks (A) after annealing at 300 °C. Incorporated Ag, therefore, delays the crystallization of TiO₂.

scan (not shown here) of a sample with no second TiO₂ layer sputtered on top of the silver. It has been shown recently²² that during reactive magnetron sputtering of transition-metal oxides, energetic oxygen ions with sufficient energy for structural modification of the growing film are present. We therefore suggest that the dispersion of the Ag layer, which is apparent from the XRD scan of the Ag–TiO₂ films, results from the impinging, energetic oxygen ions formed while the second layer of TiO₂ is sputtered. In contrast to as-deposited samples, XRD scans of films annealed at 300 and 500 °C show pronounced Ag peaks. Evidently, Ag particles have been formed inside the TiO₂ matrix, driven by the trend to minimize the Ag/TiO₂ interfacial energy. Figure 2 shows TEM photographs of a sample annealed at 300 °C with a silver film thickness equivalent of 13 nm and a total TiO₂ film thickness of 70 nm. In the cross-sectional view [Fig. 2(a)] the silver nanoparticles lined up in the TiO₂ matrix on the silicon substrate are clearly visible. As shown in the top

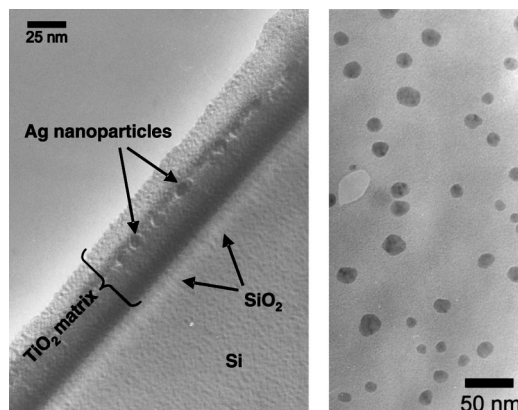


FIG. 2. TEM photographs (left: cross-section; right: top view) of Ag nanoparticles in amorphous TiO₂ annealed at 300 °C. The particles show a broad variety in shape and size, and some faceting.

view in Fig. 2(b) the particles have a broad size and shape distribution; lateral diameters varying from 10 nm up to 25 nm are estimated from the TEM picture, and the particles are partly faceted.

The XRD scan of the sample annealed at 500 °C shows another interesting aspect. The additional peaks (as compared to the sample annealed at 300 °C) show that crystallization of the TiO₂ to the anatase phase has taken place. Amorphous TiO₂ without Ag load, sputter deposited under identical conditions, would crystallize in the form of anatase after 1 h of annealing at around 300 °C, as shown in the top scan in Fig. 1 (cf. Ref. 23). In contrast, crystallization of TiO₂ loaded with Ag is delayed; according to the XRD scans, the films still remain amorphous at an annealing temperature of 450 °C (not shown here), while during annealing at 500 °C, crystallization to the anatase phase finally takes place. We understand the delayed crystallization as another indication of the fine dispersion of silver in the amorphous TiO₂ matrix during the sputter process; the presence of silver atoms appears to increase the activation barrier for crystallization. Similar phenomena have also been reported for an incorporation of Fe in TiO₂ (Ref. 24) and for sol-gel-prepared Ag-TiO₂ films.²⁵

Optical properties

Figure 3 shows optical-absorption spectra for varying annealing temperatures and Ag loads. The data shown in Fig. 3(a) for the as-deposited film show no absorption characteristic of Ag particles and thus confirm the observation made above regarding the absence of such particles. The absorption edge below 400 nm is due to interband transitions in the TiO₂, which has a band-gap energy of 3.2 eV. For the film annealed at 300 °C, a broad absorption band centered at around 550 nm is visible. It is caused by the particle-plasmon resonance of the Ag nanoparticles; this resonance is inhomogeneously broadened due to a broad distribution of particle sizes and shapes in the films, and due to possible inhomogeneities in the dielectric environment of the particles.⁹ A higher annealing temperature leads to a slight increase in absorbance, presumably due to a growth of particles at the cost of the Ag finely dispersed in the TiO₂ matrix. The maximum of the absorbance spectrum is shifted to larger wavelengths upon annealing at 500 °C, presumably due to the particle growth. It is well known that the particle-plasmon resonance is a function of particle shape and size^{10,26} and increasing particle size generally leads to a red-shift of the resonance position.^{27,28} An alternative explanation of the absorbance shift in terms of a change in the dielectric properties of the matrix cannot apply, since earlier studies²³ have shown that the change in refractive index which the TiO₂ matrix undergoes during the phase transition from the amorphous to the anatase phase is less than 2%. Mie theory²⁹ calculations for spherical particles show that a change of this order of magnitude would shift the resonance wavelength by only approximately 10 nm. Figure 3(b) shows absorbance spectra for films with various Ag loads annealed at 300 °C. At long wavelengths a strong dependence on Ag load (as given by the film thickness equivalent) is observed.

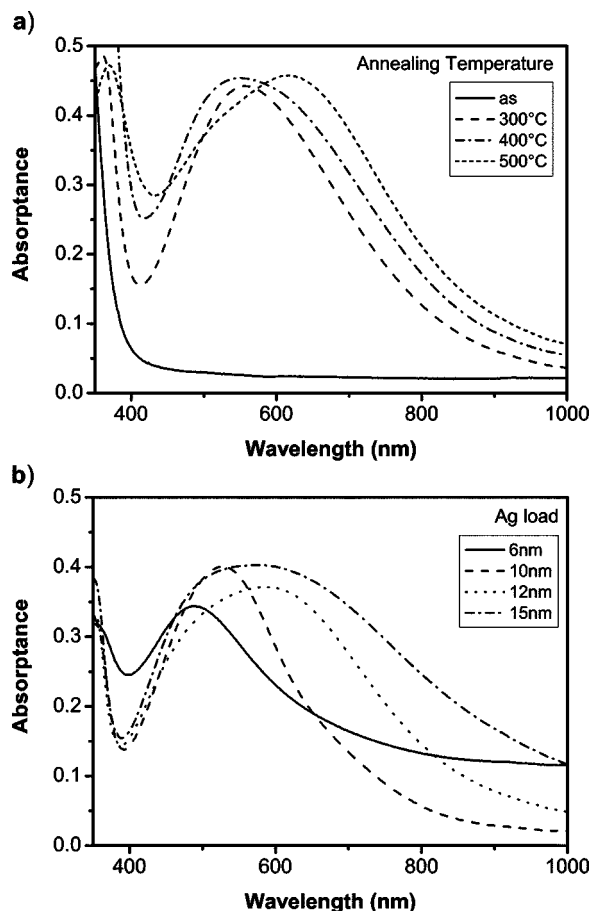


FIG. 3. Absorbance spectra of Ag-TiO₂ films with a Ag load of 13-nm film thickness equivalent, annealed at different temperatures (a) and of Ag-TiO₂ films with various silver loads annealed at 300 °C (b). The annealed films show a broad absorption band across the visible range caused by the particle-plasmon resonance of the Ag nanoparticles. Increasing the annealing temperature leads to the formation of larger particles absorbing at longer wavelengths. Similarly, the initial amount of silver present in the system allows for tuning the width and height of the absorption in the region between 500 and 800 nm.

This is consistent with the process of particle formation suggested above. The amount of silver initially present in the system determines the maximum particle size attainable and therefore controls the long-wavelength absorption of the system. Similarly, the annealing temperature controls silver aggregation into nanoparticles. Both parameters together allow the tuning of the absorption properties in the visible range.

Photochromic behavior

In the previous two sections we have demonstrated the formation of Ag nanoparticles in sputter-deposited Ag-TiO₂ nanocomposite films and analyzed the influences of annealing temperature and initial silver amount on the optical properties. In this section, the photochromic behavior is examined.

In Fig. 4 we show the change in absorbance upon laser irradiation at a wavelength of $\lambda=488$ nm, corresponding to a photon energy of 2.54 eV, and at an irradiation time of 1 h. The power density on the irradiated spots was ≈ 20 mW/mm². Samples with a Ag load of 12 nm are used for this experiment. The samples were annealed at 500 °C

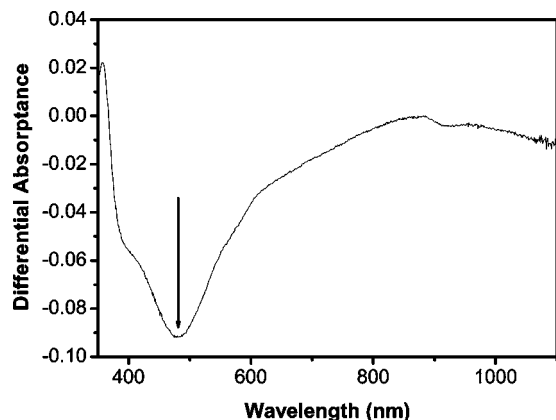


FIG. 4. Difference in absorbance (with respect to the nonilluminated state) of a Ag–TiO₂ system as described in the text after blue-green laser irradiation ($\lambda=488$ nm). A decrease of the absorbance is clearly visible at the wavelength of irradiation (arrow).

prior to laser irradiation to form a crystalline TiO₂ matrix. As a result of the laser irradiation, a deep minimum is observed in the differential absorbance spectrum at the laser wavelength (indicated by the arrow). Similar spectral holes are obtained upon laser irradiation at $\lambda=532$ nm and $\lambda=633$ nm, respectively (not shown). The intensity dependence of the spectral hole is examined by irradiating identical samples at various power densities ($\lambda=532$ nm). The irradiation time was 1 min in each case. Figure 5 shows the spectral hole depth (given as the maximum change in absorbance with respect to the nonirradiated state) for power densities between 1.5 and 47 mW/mm². The spectral hole depth increases linearly with increasing laser power density, up to a density of 15 mW/mm². At larger power densities, saturation sets in. After removal of the laser irradiation, the spectral hole gradually disappears on a time scale of several hours up to days at room temperature; the recovery time of the particle-plasmon band appears to depend on the precise preparation conditions of the samples. The recovery can be accelerated by storing the samples at elevated temperatures. Two samples irradiated at $\lambda=532$ nm and a power density of 7.5 mW/mm² were stored in an oven at 70 and 100 °C, respectively. After 1 h, the spectral hole depth of the 70 °C

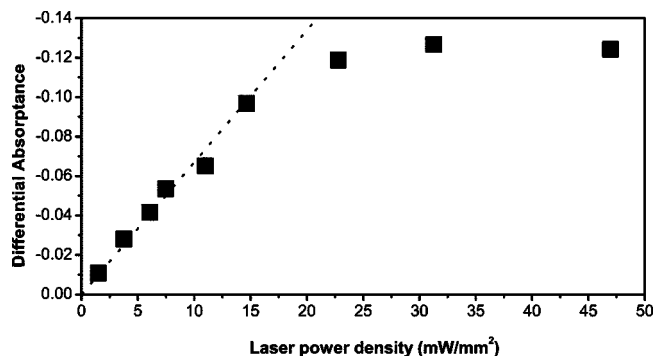


FIG. 5. Change in absorbance (with respect to the nonirradiated state) at the position of the spectral hole in a Ag–TiO₂ film after green laser irradiation at $\lambda=532$ nm for 1 min, as a function of laser power density. A linear relation between spectral hole depth and power density is observed for densities up to 15 mW/mm² (the dashed line is a guide to the eye). At larger power densities, saturation sets in.

sample was reduced by 9% as compared to the state immediately after laser irradiation, while that of the 100 °C sample was reduced by 14%.

Spectral hole burning has previously been observed by Ohko *et al.*⁸ on sol-gel Ag–TiO₂ films. They interpreted this photochromic behavior as due to photoinduced electron emission from the Ag nanoparticles. However, the precise nature of this emission has remained unclear. In the following, we wish to elucidate this point in more detail.

The linear power dependence shown in Fig. 5 indicates that the electron emission does not originate from two-photon photoemission nor higher-order multiphoton processes³⁰ but must be due to a one-photon process. Furthermore, since the laser wavelength lies in the particle-plasmon band, the incident photons will excite particle plasmons (i.e., collective oscillations of the conduction electrons in the silver nanoparticles) rather than individual electron transitions. It is well known that particle plasmons decay into other electron excitations on a time scale of a few tens of femtoseconds.^{10,28,30,31} In Ag nanoparticles these excitations occur predominantly within the conduction band, since the particle-plasmon resonance is far below the *4d-5sp* interband absorption edge of silver at 3.87 eV.³² The energy of these excitations is sufficient to promote electrons across the boundary between Ag and TiO₂ provided that the potential barrier between the two materials is low enough. The height of the Schottky barrier^{33,34} between Ag and TiO₂ may be estimated using the fact that TiO₂ shows little Fermi-level pinning.³⁵ For anatase TiO₂ films an electron affinity of 3.9 eV has been calculated from transport experiments.³⁵ Subtracting this value from the silver work function (4.3 eV, Ref. 36), we obtain a Schottky barrier height of 0.4 eV with respect to the Fermi energy in the metal. This barrier height is low enough for electrons to be promoted from the Fermi sea of silver into the conduction band of the TiO₂. This emission process results in a depletion of conduction electrons and thus a positive charging of the nanoparticles. According to simple electrostatics, the remaining conduction electrons will rearrange themselves such that a positively charged layer forms in the nanoparticles at the Ag–TiO₂ boundary. It is plausible that this layer will consist of Ag⁺ ions; indeed, the presence of Ag⁺ ions has been observed in recent x-ray photoelectron spectroscopy measurements on Ag/TiO₂ nanocomposites.²⁵ While the transformation of metallic Ag to Ag⁺ has been suggested by Ohko *et al.*⁸ to be the cause of the absorption change observed within the particle-plasmon band, the precise mechanism of this change is not entirely clear. It may be caused by a reduction of the particle-plasmon oscillator strength due to the shrinkage of the metallic Ag core and/or by a redshift of the particle-plasmon resonance frequency due to the reduced conduction electron density, as suggested by Kreibig *et al.*²⁹ and by Hilger for the case of electron transfer from Ag nanoparticles to C₆₀ acceptors.³⁷ In either case, the saturated behavior at large laser power densities in Fig. 5 indicates that the electron depletion resulting from intense or prolonged irradiation ultimately limits the electron emission from the nanoparticles. This limitation may be caused by a change in the potential barrier caused by the growth of the Ag⁺ layer.

The spectral hole burned into the inhomogeneously broadened particle-plasmon band persists for some hours up to several days after the laser irradiation has been removed. This implies that the electrons transferred from the nanoparticles to the conduction band of TiO_2 are not immediately recaptured by the positively charged particles but are trapped by some trapping centers in the TiO_2 . It is known from studies on semiconducting gas sensors that adsorbed molecular oxygen can act as an efficient trapping center for electrons in the conduction band of semiconductors.^{38,39} It is therefore likely that the trapping centers involved in the present process consist of molecular oxygen adsorbed at the surface of the thin TiO_2 film in the vicinity of the nanoparticles, resulting in the formation of O_2^- . This assumption is supported by the observation made in Ref. 8 that the spectral hole burning process strongly depends on the atmospheric environment. No spectral hole burning was observed under N_2 atmosphere.⁸ This finding can be explained with the absence of adsorbed oxygen acting as trapping centers; the emitted electrons are thus immediately recaptured by the positively charged nanoparticles during the laser irradiation. In contrast, in the presence of atmospheric oxygen, enough adsorbed oxygen is available for electron trapping. The recapture process then takes very long, since thermal release of electrons from the trapping centers to the TiO_2 conduction band will be slow at room temperature. The thermal release is expected to be accelerated at elevated temperatures; this expectation is confirmed by our observation that the recovery of the particle-plasmon band is faster at 100°C than at 70°C . Assuming that the recovery is solely limited by thermal activation of carriers from the traps to the TiO_2 conduction band rather than by transport to the, and capture into, the nanoparticles, the difference in recovery rates at the two temperatures allows us to make a rough estimate of the trap depth (with respect to the conduction-band edge), yielding ≈ 0.2 eV. This estimate is in reasonable agreement with the depth of surface trap states recently determined for polycrystalline TiO_2 films (0.185 eV).⁴⁰

We have observed that the removal of the spectral hole can be accelerated by irradiation with an ultraviolet light of 3.4-eV photon energy. A similar observation has been made by Ohko *et al.*⁸ We explain this acceleration as follows: Since the photon energy of the ultraviolet light (3.4 eV) is greater than the band-gap energy of TiO_2 (3.2 eV), electron-hole pairs are optically excited in the TiO_2 matrix. The electrons photogenerated by the ultraviolet irradiation are attracted towards the positively charged nanoparticles and captured by them. The nanoparticles are thus discharged and the particle-plasmon line is restored. Presumably the photogenerated holes will eventually recombine with the electrons that are thermally released from the oxygen trapping centers.

Figure 6 demonstrates the cyclability of the photochromic process. A spectral hole was first burned by irradiation with a red light ($\lambda=633$ nm) for 1 h. After UV irradiation ($\lambda=365$ nm), the absorption is practically restored to its original value. This photochromic cycle can be repeated by alternating irradiation at 633- and 365-nm wavelengths. The cyclability of the photochromic process in our sputter-

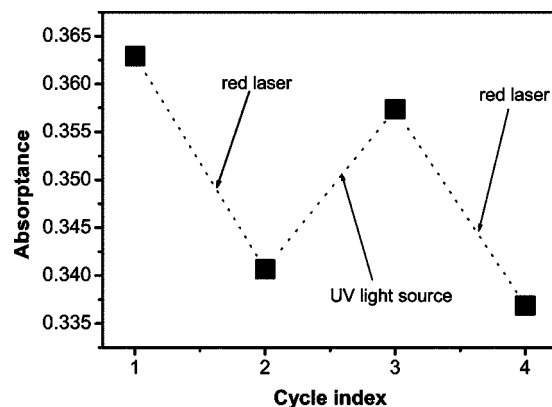


FIG. 6. The absorbance at 633 nm is recorded for a Ag-TiO_2 film irradiated with red laser light during two photochromic cycles. The repeatable effect of spectral hole burning by laser irradiation and its reversal by ultraviolet irradiation is clearly visible.

deposited Ag-TiO_2 films is thus similar to that recently demonstrated for sol-gel-processed Ag-TiO_2 films.⁸

CONCLUSION

We have presented a method for preparing photochromic Ag nanoparticles in a TiO_2 matrix using dc magnetron sputtering followed by thermal treatment. We have demonstrated that the particle-plasmon line of the Ag nanoparticles can be controlled by varying the amount of Ag present in the Ag-TiO_2 system and the annealing temperature. By irradiating the system with blue-green, green, or red laser light, spectral hole burning has been achieved. We explain the photochromic process by electron emission into the TiO_2 conduction band from those Ag nanoparticles whose particle-plasmon resonance wavelength matches the laser wavelength. The electrons are subsequently trapped by adsorbed oxygen near the Ag nanoparticles. A gradual recovery of the particle-plasmon band is observed after irradiation, which is explained with a slow thermal release of electrons from the trapping centers and subsequent capture into the nanoparticles. The recovery can be accelerated by ultraviolet irradiation; the explanation for this observation is that electrons photoexcited in the TiO_2 are captured into the nanoparticles and thus restore the absorption band.

We thank B. von Issendorf, U. Kreibig, A. Pinchuk, and D. Sanders for helpful discussions. One of the authors (J.O.) acknowledges financial support from the Alexander von Humboldt Foundation.

¹M. Lei *et al.*, Proc. SPIE **5060**, 28 (2003).

²J. N. Yao, K. Hashimoto, and A. Fujishima, Nature (London) **355**, 624 (1992).

³W. H. Armistead and S. D. Stookey, Science **140**, 150 (1964).

⁴*Persistent Spectral Hole-Burning: Science and Application*, edited by W. E. Moerner and G. C. Bjorklund (Springer, Berlin, 1988).

⁵H. W. Song and M. Nogami, J. Non-Cryst. Solids **297**, 113 (2002).

⁶J. N. Yao, P. Chen, and A. Fujishima, J. Electroanal. Chem. **102**, 1856 (1996).

⁷C. Bechinger, E. Wirth, and P. Leiderer, Appl. Phys. Lett. **68**, 2834 (1996).

⁸Y. Ohko, T. Tatsuma, T. Fujii, K. Naoi, C. Niwa, Y. Kubota, and A. Fujishima, Nat. Mater. **2**, 29 (2003).

⁹K. Naoi, Y. Ohko, and T. Tatsuma, J. Am. Chem. Soc. **126**, 3664 (2004).

- ¹⁰U. Kreibig and M. Vollmer, *Optical Properties of Metal Clusters* (Springer, Berlin, 1995).
- ¹¹S. Nie and S. R. Emory, *Science* **275**, 1102 (1997).
- ¹²N. Nilius, N. Ernst, and H. J. Freund, *Phys. Rev. Lett.* **84**, 3994 (2000).
- ¹³L. A. Peyser, A. E. Vinson, A. P. Bartko, and R. M. Dickson, *Science* **291**, 103 (2001).
- ¹⁴S. Takeda, S. Suzuki, H. Odaka, and H. Hosono, *Thin Solid Films* **392**, 338 (2001).
- ¹⁵S. Sakka and H. Kozuka, *J. Sol-Gel Sci. Technol.* **13**, 701 (1998).
- ¹⁶P. Innocenzi, G. Brusatin, A. Martucci, and K. Urab, *Thin Solid Films* **279**, 23 (1996).
- ¹⁷C. M. Wang, Y. Zhang, V. Shutthanandan, S. Thevuthasan, and G. Duscher, *J. Appl. Phys.* **95**, 8185 (2004).
- ¹⁸H. B. Liao, R. F. Xiao, H. Wang, K. S. Wong, and G. K. L. Wong, *Appl. Phys. Lett.* **72**, 1817 (1998).
- ¹⁹M. Radecka, A. Gorzkowska-Sobaś, K. Zakrzewska, and P. Sobaś, *Opto-Electron. Rev.* **12**, 53 (2004).
- ²⁰R. D. Arnell and P. J. Kelly, *Surf. Coat. Technol.* **112**, 170 (1999).
- ²¹E. Hecht, *Optics*, 2nd ed. (Addison-Wesley, Reading, MA, 1987).
- ²²J. M. Ngaruiya, O. Kappertz, S. H. Mohamed, and M. Wuttig, *Appl. Phys. Lett.* **85**, 748 (2004).
- ²³S. M. Mohamed, O. Kappertz, T. P. L. Pedersen, R. Drese, and M. Wuttig, *Phys. Status Solidi A* **198**, 224 (2003).
- ²⁴W. Zhang, Y. Li, S. Zhu, and F. Wang, *Chem. Phys. Lett.* **373**, 333 (2003).
- ²⁵E. Traversa, M. L. di Vona, P. Nunziante, S. Licocchia, J. W. Yoon, T. Sasaki, and N. Koshizaki, *J. Sol-Gel Sci. Technol.* **22**, 115 (2001).
- ²⁶S. Link and M. A. El-Sayed, *J. Phys. Chem. B* **103**, 8410 (1999).
- ²⁷J. H. Hodak, A. Henglein, and G. V. Hartland, *J. Chem. Phys.* **111**, 8613 (1999).
- ²⁸C. Sönnichsen, T. Franzl, T. Wilk, G. von Plessen, J. Feldmann, O. Wilson, and P. Mulvaney, *Phys. Rev. Lett.* **88**, 77402 (2002).
- ²⁹U. Kreibig, M. Gartz, and A. Hilger, *Ber. Bunsenges. Phys. Chem.* **101**, 1593 (1997).
- ³⁰J. Lehmann, M. Merschedorf, W. Pfeiffer, A. Thon, S. Voll, and G. Gerber, *Phys. Rev. Lett.* **85**, 2921 (2000).
- ³¹C. Sönnichsen, T. Franzl, T. Wilk, G. von Plessen, and J. Feldmann, *New J. Phys.* **4**, 93 (2002).
- ³²F. Abelès, *Optical Properties of Solids* (North-Holland, Amsterdam, 1972).
- ³³A. Wood, M. Giersig, and P. Mulvaney, *J. Phys. Chem. B* **105**, 8810 (2001).
- ³⁴M. Jakob, H. Levanon, and P. V. Kamat, *Nano Lett.* **3**, 353 (2003).
- ³⁵R. Könenkamp, *Phys. Rev. B* **61**, 11057 (2000).
- ³⁶*Handbook of Thermionic Properties*, edited by G. Samsonov (Plenum, New York, 1968).
- ³⁷A. Hilger, Ph.D. thesis, Rheinisch-Westfälische Technische Hochschule Aachen (2001).
- ³⁸N. Yamazoe, *Sens. Actuators B* **5**, 7 (1991).
- ³⁹N. Barsan, M. Schweizer-Berberich, and W. Göpel, *J. Anal. Chem. USSR* **365**, 287 (1999).
- ⁴⁰Q. Fan, B. McQuillin, A. K. Ray, M. L. Turner, and A. B. Seddon, *J. Phys. D* **33**, 2683 (2000).